

Supporting Information

Structure and Nuclease Resistance of 2',4'-Constrained 2'-*O*-Methoxyethyl (cMOE) and 2'-*O*-Ethyl (cEt) Modified DNAs

Pradeep S. Pallan,^a Charles R. Allerson,^b Andres Berdeja,^b Punit P. Seth,^b Eric E. Swayze,^b Thazha P. Prakash^b and Martin Egli*^a

^a *Department of Biochemistry, Vanderbilt University School of Medicine, Nashville, TN 37232, USA.*

^b *Department of Medicinal Chemistry, Isis Pharmaceuticals, 2855 Gazelle Court, Carlsbad, CA 92010, USA.*

*E-mail: martin.egli@vanderbilt.edu; Fax: 1-615-322-7122; Tel: 1-615-343-8070.

Supporting Information Contents

Page S2	Nuclease stability of DNA, MOE, LNA, cEt BNA and cMOE BNA modified oligonucleotide phosphodiester, Table S1
Page S2	Crystallization experiments
Page S3	X-ray data collection, structure determination and refinement
Page S4	Table S2. Selected crystal data and refinement parameters
Page S5	Figure S1. Electron density and overall structure of duplexes
Page S6	Figure S2. Origins of the improved nuclease resistance of cEt/cMOE BNA
Page S8	References

Nuclease stability of DNA, MOE, LNA, cEt BNA and cMOE BNA modified oligonucleotide phosphodiesteres

The nuclease stability of oligonucleotides containing DNA, MOE, LNA, cEt BNA and cMOE BNA modifications was determined using snake venom phosphodiesterase (SVPD). Each oligonucleotide was prepared as a 500 μ L mixture containing: 12.5 μ L 200 μ M oligomer, 50 μ L SVDP at 0.005 Units/mL in SVDP buffer (50 mM Tris-HcL, pH 7.5, 8 mM MgCl₂) final concentration 0.0005 Units/mL, 438.5 μ L SVP buffer. Samples were incubated at 37°C in a thermoblock. Aliquots (50 μ L) were taken at different intervals. EDTA was added to aliquots immediately after removal to quench enzyme activity and the samples were analyzed on IP HPLC/MS. The results are expressed as half-time ($T_{1/2}$) and presented in **Table S1**.

Table S1. 3'-Exonuclease stability of DNA, MOE, LNA, cEt BNA and cMOE BNA modified oligonucleotide phosphodiesteres

No.	Sequence	Chemistry*	$T_{1/2}$ (min)
1	5'-TTTTTTTTTTTTT -3'	DNA	0.6
2	5'-TTTTTTTTTTTTT _e T _e -3'	MOE	4.3
3	5'-TTTTTTTTTTTTT _T T _T -3'	LNA	3.0
4	5'-TTTTTTTTTTTTT _{x1} T _{x1} -3'	(S)-cEt BNA	840
5	5'-TTTTTTTTTTTTT _{x2} T _{x2} -3'	(R)-cEt BNA	>1200
6	5'-TTT TTTTTTTU ₁ U ₁ -3'	LNA	4.8
7	5'-TTTTTTTTTTTU _{x3} U _{x3} -3'	(S)-cMOE BNA	>1200
8	5'-TTTTTTTTTTTU _{x4} U _{x4} -3'	(R)-cMOE BNA	>1200

*T_e = 2'-O-MOE T; T_T = LNA T; T_{x1} = (S)-cEt BNA T; T_{x2} = (R)-cEt BNA T; U_{x3} = (S)-cMOE BNA U; U_{x4} = (R)-cMOE BNA U

Crystallization experiments

The three DNA decamers d(GCGTAU*ACGC), U* = (*R*)-cEt BNA, (*S*)-cEt BNA, or (*S*)-cMOE BNA, were synthesized as described previously¹ and purified by ion exchange chromatography. The stock concentrations for all three strands were adjusted to ca. 1.2 mM and crystallization trials were performed by the hanging drop vapor diffusion technique, using the 24 conditions of the Nucleic Acid Miniscreen (Hampton Research Inc., Aliso Viejo, CA).² The reservoir solution was 800 μ L of a 35% v/v solution of 2-methyl-2,4-pentanediol (MPD). Droplets (1 μ L) of modified DNA decamer solutions were mixed with droplets of equal volume of the individual sparse matrix screen solutions and equilibrated against MPD at room temperature. The optimal crystallization conditions for the three oligonucleotides were as follows. (*R*)-cEt BNA: condition 8, 40 mM sodium cacodylate, pH 6.0, 80 mM sodium chloride, 12 mM spermine tetrahydrochloride, and 10% v/v MPD. (*S*)-cEt BNA: condition 19, 40 mM sodium cacodylate, pH 7.0, 12 mM sodium chloride, 80 mM potassium chloride, 12 mM spermine tetrahydrochloride, and 10% v/v MPD. (*S*)-cMOE BNA: condition 10, 40 mM sodium cacodylate, pH 6.0, 12 mM sodium chloride, 80 mM potassium chloride, 12 mM spermine tetrahydrochloride, and 10% v/v MPD.

X-ray data collection, structure determination and refinement

Crystals were mounted in nylon loops, flash-frozen in liquid nitrogen without further cryoprotection and stored in liquid nitrogen prior to data collection. Data for (*S*)-cEt BNA crystal were collected on the 21-ID-F beam line of the Life Sciences Collaborative Access Team (LS-CAT) at the Advanced Photon Source (APS), located at Argonne National Laboratory (Argonne, IL) using a MARCCD 225 detector, at a wavelength of 0.98 Å. The data sets for (*R*)-cEt BNA and (*S*)-cMOE BNA were collected on the 21-ID-D beam line of LS-CAT using a MARCCD 300 detector at a wavelength of 1.007 Å. In all three cases, the crystals were kept at 110 K during data collection. Diffraction data were integrated, scaled and merged with HKL2000.³ Selected crystal data and diffraction data statistics are listed in **Table S2**. The structures were determined by the molecular replacement method with the program Molrep⁴ in the CCP4 suite of crystallographic software,⁵ using an A-form DNA as the search model (PDB ID 3EY2⁶). Following initial positional and isotropic temperature factor refinement cycles with the program Refmac,⁷ the chemically modified uridines were built into Fourier ($2F_o - F_c$) sum and ($F_o - F_c$) difference electron density maps visualized either with Turbo-Frodo⁸ or Coot.⁹ Following adaptation of the dictionary files, refinement was continued and all nucleic acid atoms and water molecules were treated with anisotropic B-factors.¹⁰ Final refinement statistics are summarized in **Table S1**. Helical parameters were calculated with the program Curves¹¹ and the illustrations of the two base-pair steps and the overall structures shown in **Figure S1** were generated with the program UCSF Chimera.¹²

Table S2. Selected crystal data and refinement parameters

Oligonucleotide Sequence	d(GCGTAU*ACGC)		
	(R)-cEt BNA	(S)-cEt BNA	(S)-cMOE BNA
Modified nucleotide (U*)			
Space group		Orthorhombic $P2_12_12_1$	
Unit cell constants [Å] $\alpha=\beta=\gamma=90^\circ$	$a=26.02$ $b=44.90$ $c=44.91$	$a=26.13$ $b=44.01$ $c=45.53$	$a=24.49$ $b=44.66$ $c=46.60$
Resolution [Å]	1.42	1.54	1.68
Outer shell [Å]	1.47-1.42	1.60-1.54	1.74-1.68
Number of unique reflections	10,325	8,177	6,270
Completeness (outer shell) [%]	99.4 (94.5)	99.6 (98.5)	100.0 (100.0)
R-merge (outer shell) [%]	0.062 (0.505)	0.053 (0.433)	0.096 (0.616)
R-work [%]	0.146	0.176	0.181
R-free [%]	0.208	0.215	0.250
No. of DNA atoms	408	408	412
No. of waters	85	53	57
R.m.s.d. bonds [Å]	0.024	0.013	0.011
R.m.s.d. angles [°]	2.4	2.6	2.3
Avg. B-factor, DNA atoms [Å ²]	14.5	23.4	22.3
Avg. B-factor, solvent [Å ²]	25.9	37.3	31.3
PDB ID code	3UKB	3UKC	3UKE

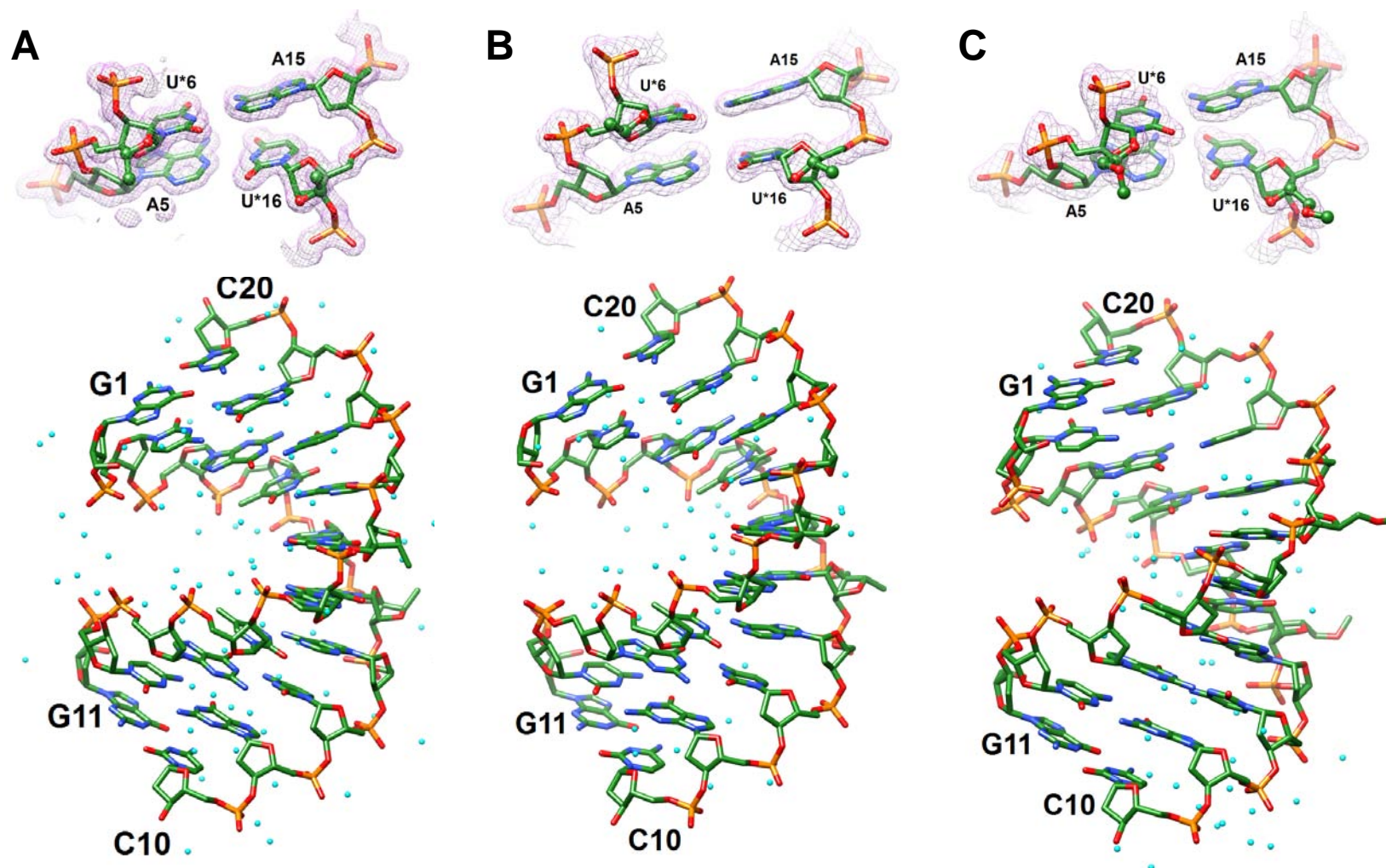


Figure S1. Examples of the quality of the final Fourier ($2F_o - F_c$) sum electron density ($\sim 1.1 \sigma$ threshold) and the overall structures of *(R)*-cEt BNA, *(S)*-cEt BNA and *(S)*-c MOE BNA duplexes. Electron density around (top panel) and overall structure (bottom panel) of **(A)** the *(R)*-cEt BNA duplex, **(B)** the *(S)*-cEt BNA duplex, and **(C)** the *(S)*-cMOE BNA duplex. The view is across the grooves, DNA atoms are colored green, red, blue and orange for carbon, oxygen, nitrogen and phosphorus, respectively, and water molecules are cyan spheres.

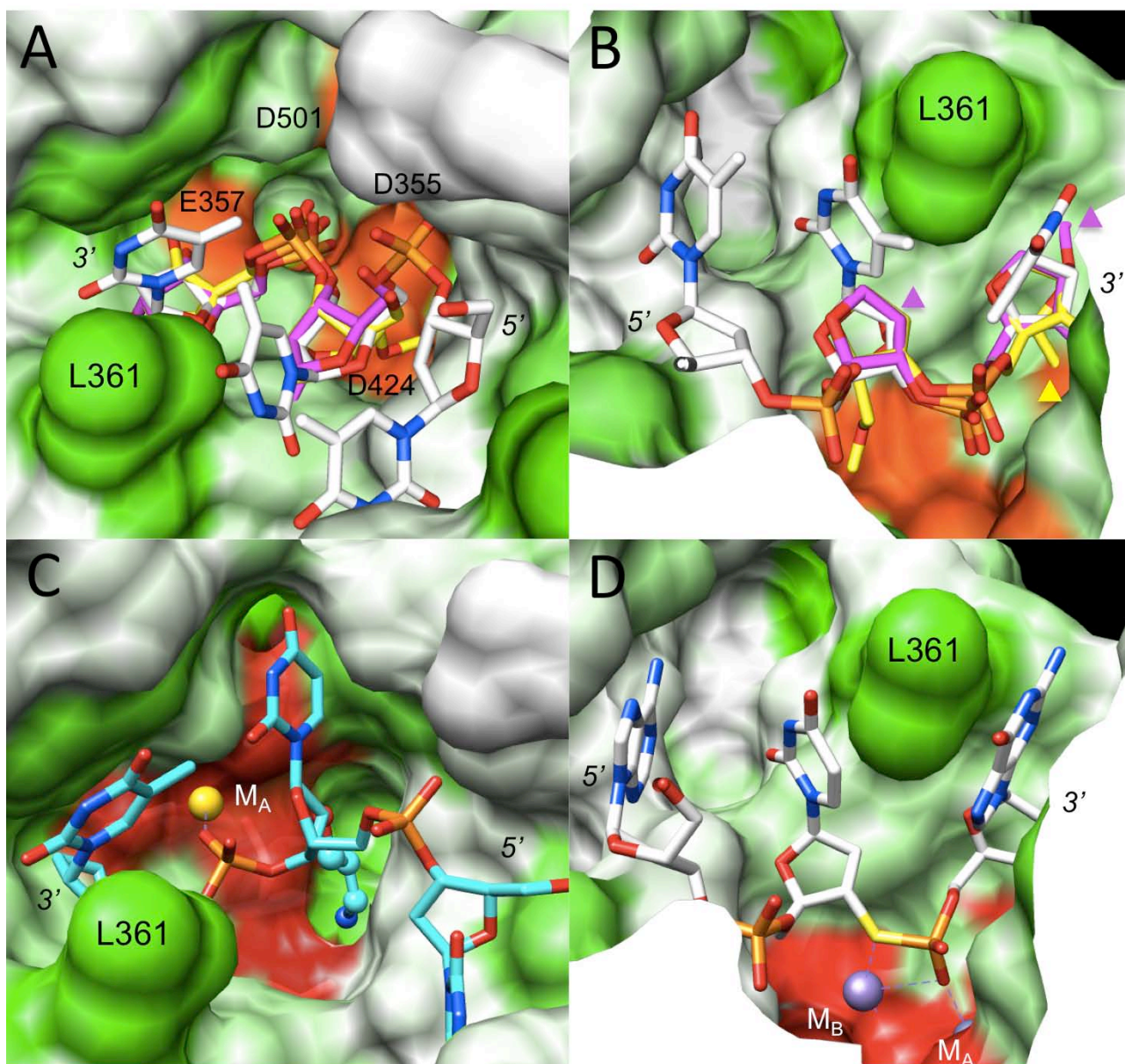


Figure S2. Orientation of oligonucleotides at the *E. coli* DNA polymerase I Klenow fragment (Kf) 3'-5' exonucleolytic active site. The enzyme is shown in a surface representation and is colored according to hydrophobicity: white=least hydrophobic, and green=most hydrophobic. The surface around residues D424, D355 (D355A mutation in panels A and B), E357 (D357A mutation in panels A and B) and D501 that serve the binding of metal ion cofactors are colored in red. (A) Crystal structure of the complex between the D355A/E357A Kf mutant and dT₁₉ (white carbon atoms; PDB ID 1D8Y).¹³ Only the three nucleotides at the 3'-terminal end were visualized in the structure. Superimposition of a 2'-O-MOE RNA dinucleotide (taken from the structure of an all-

modified 12mer, PDB ID 469D)¹⁴ onto TT-3' results in 2'-*O*-MOE substituents penetrating the surface, thus indicating clashes with protein residues. Only the sugar-phosphate backbone is shown for the 2'-MOE-RNA dimer, with carbon atoms colored in magenta. By comparison, superimposition of an (*S*)-cMOE BNA-modified dimer (yellow carbons) onto TT-3' reveals a radically different orientation of 2'-cMOE relative to 2'-*O*-MOE substituents. The cMOE substituent of the penultimate nucleotide can be seen to reach into the metal ion B coordination site; metal ion cofactors are absent in this structure of the Kf double mutant. **(B)** The active site in panel A viewed approximately from the opposite side, with the scissile phosphate and the cMOE substituent of the penultimate nucleotide visible at the bottom right. Sites where MOE and cMOE substituents dip into the surface are marked by magenta and yellow triangles, respectively. **(C)** Crystal structure of the complex between wt-Kf and 5'-d(TTU**T*) (cyan carbon atoms; U* = 2'-*O*-(3-aminopropyl)-U); PDB ID 1D9F).¹³ Only the three nucleotides at the 3'-terminal end were visualized in the structure, atoms of the 2'-substituent are highlighted in ball-and-stick mode, and the metal ion bound at site A is shown as a golden sphere. **(D)** Crystal structure of the complex between wt-Kf and 5'-d(GCTTAU**G*) (U* = 3'-phosphorothiolate-U) in the presence of Zn²⁺ (M_A) and Mn²⁺ (M_B, slightly obscured) (PDB ID 2KFN).¹⁵ Only the three nucleotides at the 3'-terminal end were visualized in the structure and metal ions are shown as purple spheres.

Because the views into the active site in panels A and C are roughly the same, it is evident that the orientations and conformations of the TTT and TU**T* trimers in the structures of mt-Kf and wt-Kf, respectively, are quite different. In the latter structure, the 2'-*O*-(3-aminopropyl) substituent displaces metal ion B (see also panel D for the locations of metal ions A and B) and forms a salt bridge with D424, thereby providing a rationalization for the superior protection against degradation by exonucleases afforded by the zwitterionic modification.¹⁵ Interestingly, the cMOE substituent of the penultimate residue (panels A, B) reaches into a very similar area (see panel C for comparison) and, unlike MOE, may also lead to displacement of a metal ion. Although steric hindrance will protect against degradation to various degrees,¹⁶ we hypothesize that a modification that generates a steric challenge to nuclease binding *and* interferes with the metal ion cofactor(s), as seen here in the cMOE BNA model, should provide superior protection against degradation.

References

1. Seth, P. P.; Vasquez, G.; Allerson, C. A.; Berdeja, A.; Gaus, H.; Kinberger, G. A.; Prakash, T. P.; Migawa, M. T.; Bhat, B.; Swayze, E. E. *J. Org. Chem.* **2010**, *75*, 1569-81.
2. Berger, I.; Kang, C. H.; Sinha, N.; Wolters, M.; Rich, A. *Acta Cryst. D* **1996**, *52*, 465-468.
3. Otwinowski, Z.; Minor, W. *Meth. Enzymol.* **1997**, *276*, 307-326.
4. Vagin, A.; Teplyakov, A. *J. Appl. Crystallogr.* **1997**, *30*, 1022-1025.
5. Collaborative Computational Project, Number 4. The CCP4 suite: programs for protein crystallography. *Acta Cryst. D*, **1994**, *50*, 760-763.
6. Pallan, P. S.; Prakash, T. P.; Li, F.; Eoff, R. L.; Manoharan, M.; Egli, M. *Chem. Comm.* **2009**, 2017-2019.
7. Murshudov, G. N.; Vagin, A. A.; Dodson, E. J. *Acta Cryst. D* **1997**, *53*, 240-255.
8. Cambillau, C.; Roussel, A. Turbo Frodo, **1997**, Version OpenGL.1.
9. Emsley, P.; Cowtan, K. *Acta Cryst. D* **2004**, *60*, 2126-2132.
10. Winn, M. D.; Isupov, M. N.; Murshudov, G. N. *Acta Cryst. D* **2001**, *57*, 122-133.
11. Lavery, R.; Sklenar, H. *J. Biomol. Struct. Dyn.* **1989**, *6*, 655-667.
12. Pettersen, E. F.; Goddard, T. D.; Huang, C. C.; Couch, G. S.; Greenblatt, D. M.; Meng, E. C.; Ferrin, T. E. *J. Comp. Chem.* **2004**, *25*, 1605-1612.
13. Teplova, M.; Wallace, S. T.; Minasov, G.; Tereshko, V.; Symons, A.; Cook, P. D.; Manoharan, M.; Egli, M. *Proc. Natl. Acad. Sci. U.S.A.* **1999**, *96*, 14240-14245.
14. Teplova, M.; Minasov, G.; Tereshko, V.; Inamati, G. B.; Cook, P. D.; Manoharan, M.; Egli, M. *Nat. Struct. Biol.*, **1999**, *6*, 535-539.
15. Brautigam, C. A.; Sun, S.; Piccirilli, J. A.; Steitz, T. A. *Biochemistry* **1999**, *38*, 696-704.
16. Egli, M.; Minasov, G.; Tereshko, V.; Pallan, P. S.; Teplova, M.; Inamati, G. B.; Lesnik, E. A.; Owens, S. R.; Ross, B. S.; Prakash, T. P.; Manoharan, M. *Biochemistry* **2005**, *44*, 9045-9057.